CHAPTER 13

COMBUSTION OF SOLID PROPELLANTS

This is the third of four chapters on solid propellant motors. We discuss the combustion of solid propellants, the physical and chemical processes of burning, the ignition or startup process, the extinction of burning, and combustion instability.

The combustion process in rocket propulsion systems is very efficient, when compared to other power plants, because the combustion temperatures are very high; this accelerates the rate of chemical reaction, helping to achieve nearly complete combustion. As was mentioned in Chapter 2, the energy released in the combustion is between 95 and 99.5% of the possible maximum. This is difficult to improve. There has been much interesting research on rocket combustion and we have now a better understanding of the phenomena and of the behavior of burning propellants. This combustion area is still the domain of specialists. The rocket motor designers have been concerned not so much with the burning process as with controlling the combustion (start, stop, heat effects) and with preventing the occurrence of combustion instability.

13.1. PHYSICAL AND CHEMICAL PROCESSES

The combustion in a solid propellant motor involves exceedingly complex reactions taking place in the solid, liquid, and gas phases of a heterogeneous mixture. Not only are the physical and chemical processes occurring during solid propellant combustion not fully understood, but the available analytical combustion models remain oversimplified and unreliable. Experimental observations of burning propellants show complicated three-dimensional micro-

structures, a three-dimensional flame structure, intermediate products in the liquid and gaseous phase, spatially and temporally variant processes, aluminum agglomeration, nonlinear response behavior, formation of carbon particles, and other complexities yet to be adequately reflected in mathematical models.

Some insight into this combustion process can be gained by understanding the behavior of the major ingredients, such a ammonium perchlorate, which is fairly well explored. This oxidizer is capable of self-deflagration with a low-pressure combustion limit at approximately 2 MPa, the existence of at least four distinct "froth" zones of combustion between 2 and 70 MPa, the existence of a liquid froth on the surface of the crystal during deflagration between 2 and 6 MPa, and a change in the energy-transfer mechanism (particularly at about 14 MPa). Its influence on combustion is critically dependent on oxidizer purity. The surface regression rate ranges from 3 mm/sec at 299 K and 2 MPa to 10 mm/sec at 423 K and 1.4 MPa.

The various polymeric binders used in composite propellants are less well characterized and their combustion properties vary, depending on the binder type, heating rate, and combustion chamber pressure.

The addition of powdered aluminum (2 to 40 μm) is known to favorably influence specific impulse and combustion stability. Photography of the burning aluminum particles shows that the particles usually collect into relatively large accumulaties (100 or more particles) during the combustion process. The combustion behavior of this ingredient depends on many variables, including particle size and shape, surface oxides, the binder, and the combustion wave environment. Ref. 13–1 describes solid propellant combustion.

Visual observations and measurements of flames in simple experiments, such as strand burner tests, give an insight into the combustion process. For double-base propellants the combustion flame structure appears to be homogeneous and one-dimensional along the burning direction, as shown in Fig. 13–1. When heat from the combustion melts, decomposes, and vaporizes the solid propellant at the burning surface, the resulting gases seem to be already premixed. One can see a brilliantly radiating bright flame zone where most of the chemical reaction is believed to occur and a dark zone between the bright flame and the burning surface. The brightly radiating hot reaction zone seems to be detached from the combustion surface. The combustion that occurs inside the dark zone does not emit strong radiations in the visible spectrum, but does emit in the infrared spectral region. The dark zone thickness decreases with increasing chamber pressure, and higher heat transfer to the burning surface causes the burning rate to increase. Experiments on strand burners in an inert nitrogen atmosphere, reported in Chapter 1 of Ref. 13–1, show this dramatically: for pressures of 10, 20, and 30 atm the dark zone thickness is 12, 3.3, and 1.4 mm, respectively, and the corresponding burning rates are 2.2, 3.1, and 4.0 mm/sec. The overall length of the visible flame becomes shorter as the chamber pressure increases and the heat release per unit volume near the surface also increases. In the bright, thin fizz zone or combustion zone directly over the burning surface of the DB propellant, some burning and heat release occurs. Beneath

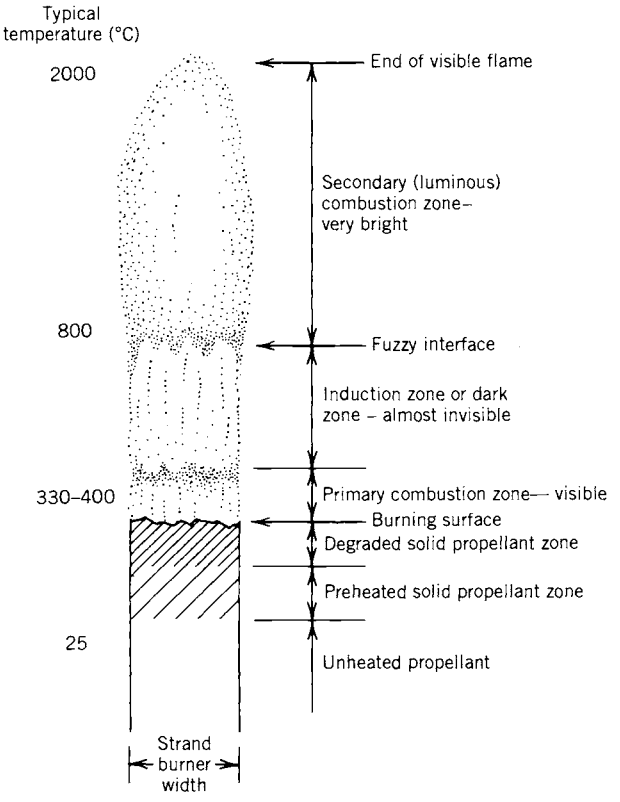

FIGURE 13–1. Schematic diagram of the combustion flame structure of a double-base propellant as seen with a strand burner in an inert atmosphere. (Adapted from Chapter 1 of Ref. 13–1 with permission of the American Institute of Aeronautics and Astronautics, AIAA.)

is a zone of liquefied bubbling propellant which is thought to be very thin (less than 1 μm) and which has been called the foam or degradation zone. Here the temperature becomes high enough for the propellant molecules to vaporize and break up or degrade into smaller molecules, such as NO_2, aldehydes, or NO, which leave the foaming surface. Underneath is the solid propellant, but the layer next to the surface has been heated by conduction within the solid propellant material.

Burn rate catalysts seem to affect the primary combustion zone rather than the processes in the condensed phase. They catalyze the reaction at or near the surface, increase or decrease the heat input into the surface, and change the amount of propellant that is burned.

A typical flame for an AP/Al/HTPB* propellant looks very different, as seen in Fig. 13–2. Here the luminous flame seems to be attached to the burning

*Acronyms are explained in Tables 12–6 and 12–7.

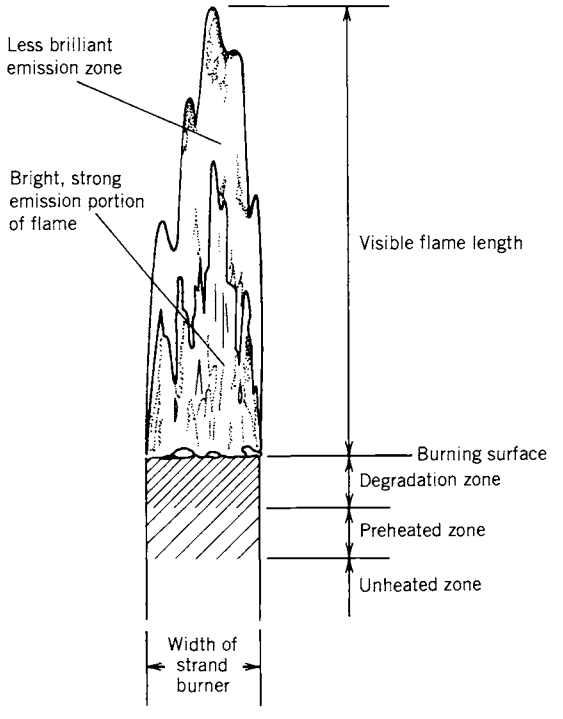

FIGURE 13–2. Diagram of the flickering, irregular combustion flame of a composite propellant (69% AP, 19% Al, plus binder and additives) in a strand burner with a neutral atmosphere. (Adapted from Chapter 1 of Ref. 13–1 with permission of AIAA.)

surface, even at low pressures. There is no dark zone. The oxidizer-rich decomposed gases from the AP diffuse into the fuel-rich decomposed gases from the fuel ingredients, and vice versa. Some solid particles (aluminum, AP crystals, small pieces of binder, or combinations of these) break loose from the surface and the particles continue to react and degrade while in the gas flow. The burning gas contains liquid particles of hot aluminum oxides, which radiate intensively. The propellant material and the burning surface are not homogeneous. The flame structure is unsteady (flicker), three dimensional, not truly axisymmetrical, and complex. The flame structure and the burning rates of composite-modified cast double-base (CMDB) propellant with AP and Al seem to approach those of composite propellant, particularly when the AP content is high. Again there is no dark zone and the flame structure is unsteady and not axisymmetrical. It also has a complex three-dimensional flame structure.

According to Ref. 13–1, the flame structure for double-base propellant with a nitramine addition shows a thin dark zone and a slightly luminous degradation zone on the burning surface. The dark zone decreases in length with increasd pressure. The decomposed gases of RDX or HMX are essentially

neutral (not oxidizing) when decomposed as pure ingredients. In this CMDB/RDX propellant the degradation products of RDX solid crystals interdiffuse with the gas from the DB matrix just above the burning surface, before the RDX particles can produce monopropellant flamelets. Thus an essentially homogeneous premixed gas flame is formed, even though the solid propellant itself is heterogeneous. The flame structure appears to be one-dimensional. The burning rate of this propellant decreases when the RDX percentage is increased and seems to be almost unaffected by changes in RDX particle size. Much work has been done to characterize the burning behavior of different propellants. See Chapters 2, 3, and 4 by Kishore and Gayathri, Boggs, and Fifer, respectively, in Ref. 13–1, and Refs. 13–2 to 13–8.

The burning rate of all propellants is influenced by pressure (see Section 11.1 and Eq. 11–3), the initial ambient solid propellant temperature, the burn rate catalyst, the aluminum particle sizes and their size distribution, and to a lesser extent by other ingredients and manufacturing process variables. Erosive burning is basically an accelerated combustion phenomenon stimulated by increased heat transfer and erosion by local high velocities; this was discussed briefly in Chapter 11. Analysis of combustion is treated later in this chapter.

13.2. IGNITION PROCESS

This section is concerned with the mechanism or the process for initiating the combustion of a solid propellant grain. Specific propellants that have been successfully used for igniters have been mentioned in Section 12.5. The hardware, types, design, and integration of igniters into the motor are described in Section 14.4. Chapters 2, 5, and 6 of Ref. 13–1 review the state of the art of ignition, data from experiments, and analytical models, which have been found to be mostly unreliable.

Solid propellant ignition consists of a series of complex rapid events, which start on receipt of a signal (usually electric) and include heat generation, transfer of the heat from the igniter to the motor grain surface, spreading the flame over the entire burning surface area, filling the chamber free volume (cavity) with gas, and elevating the chamber pressure without serious abnormalities such as overpressures, combustion oscillations, damaging shock waves, hangfires (delayed ignition), extinguishment, and chuffing. The *igniter* in a solid rocket motor generates the heat and gas required for motor ignition.

Motor ignition must usually be complete in a fraction of a second for all but the very large motors (see Ref. 13–9). The motor pressure rises to an equilibrium state in a very short time, as shown in Fig. 13–3. Conventionally, the ignition process is divided into three phases for analytical purposes:

Phase I, *Ignition time lag*: the period from the moment the igniter receives a signal until the first bit of grain surface burns.

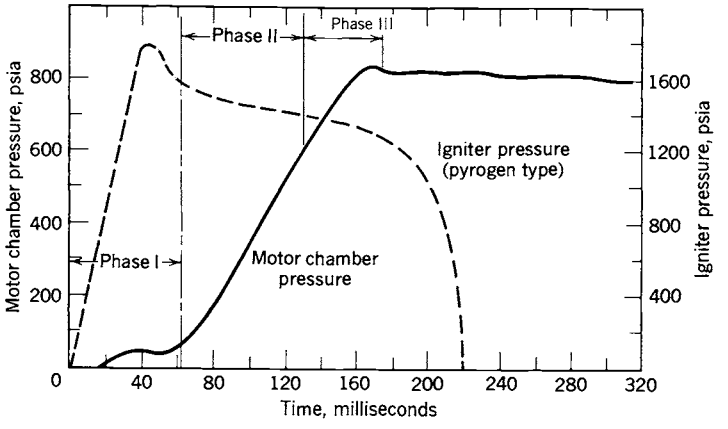

FIGURE 13–3. Typical ignition pressure transient portion of motor chamber pressure–time trace with igniter pressure trace and ignition process phases shown. Electric signal is received a few milliseconds before time zero.

Phase II, *Flame-spreading interval*: the time from first ignition of the grain surface until the complete grain burning area has been ignited.

Phase III, *Chamber-filling interval*: the time for completing the chamber-filling process and for reaching equilibrium chamber pressure and flow.

The ignition will be successful once enough grain surface is ignited and burning, so that the motor will continue to raise its own pressure to the operating chamber pressure. The critical process seems to be a gas-phase reaction above the burning surface, when propellant vapors or decomposition products interact with each other and with the igniter gas products. If the igniter is not powerful enough, some grain surfaces may burn for a short time, but the flame will be extinguished.

Satisfactory attainment of equilibrium chamber pressure with full gas flow is dependent on (1) characteristics of the igniter and the gas temperature, composition and flow issuing from the igniter, (2) motor propellant composition and grain surface ignitability, (3) heat transfer characteristics by radiation and convection between the igniter gas and grain surface, (4) grain flame spreading rate, and (5) the dynamics of filling the motor free volume with hot gas (see Ref. 13–10). The quantity and type of caloric energy needed to ignite a particular motor grain in the prevailing environment has a direct bearing on most of the igniters' design parameters—particularly those affecting the required heat output. The ignitability of a propellant at a given pressure and temperature is normally shown as a plot of ignition time versus heat flux received by the propellant surface, as shown in Fig. 13–4; these data are obtained from laboratory tests. Ignitability of a propellant is affected by many factors, including (1) the propellant formulation, (2) the initial temperature of the propellant grain

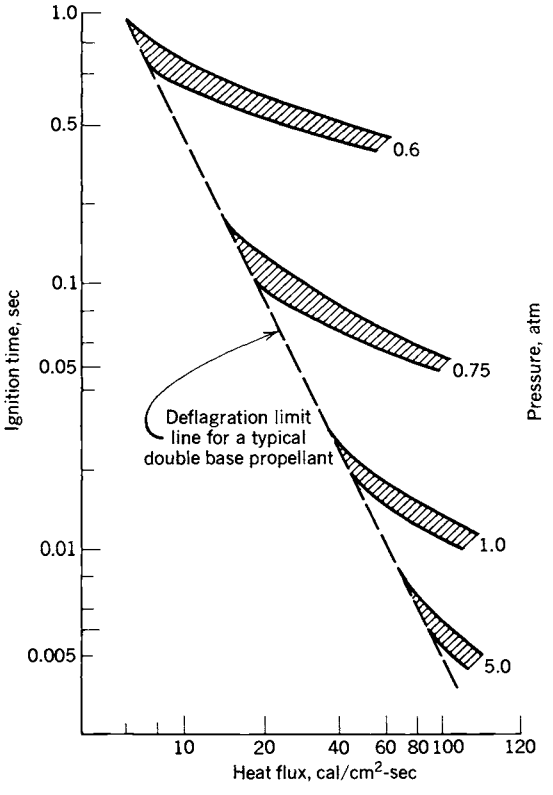

FIGURE 13–4. Propellant ignitability curves: effect of heat flux on ignition time for a specific motor.

surface, (3) the surrounding pressure, (4) the mode of heat transfer, (5) grain surface roughness, (6) age of the propellant, (7) the composition and hot solid particle content of the igniter gases, (8) the igniter propellant and its initial temperature, (9) the velocity of the hot igniter gases relative to the grain surface, and (10) the cavity volume and configuration. Figure 13–4 and data in Chapter 14 show that the ignition time becomes shorter with increases in both heat flux and chamber pressure. If a short ignition delay is required, then a more powerful igniter will be needed. The radiation effects can be significant in the ignition transient as described in Ref. 13–11. In Section 14.3 we describe an analysis and design for igniters.

13.3. EXTINCTION OR THRUST TERMINATION

Sometimes it is necessary to stop or extinguish the burning of a solid motor before all the propellant has been consumed:

1. When a flight vehicle has reached the desired flight velocity (for a ballistic missile to attain a predetermined velocity or for a satellite to achieve an accurate orbit), or a precise total impulse cutoff is needed.
2. As a safety measure, when it appears that a flight test vehicle will unexpectedly fly out of the safe boundaries of a flight test range facility.
3. To avoid collisions of stages during a stage separation maneuver (requiring a thrust reversal) for multistage flight vehicles.
4. During research and development testing, when one wants to examine a partially burned motor.

The common mechanisms for achieving extinction are listed below and described in Chapters 2, 5, and 6 of Ref. 13–1.

1. Very *rapid depressurization*, usually by a sudden, large increase of the nozzle throat area or by fast opening of additional gas escape areas or ports. The most common technique neutralizes the thrust or reverses the net thrust direction by suddenly opening exhaust ports in the forward end of the motor case. Such a thrust reversal using ports located on the forward bulkhead of the case is achieved in the upper stages of Minuteman and Poseidon missiles. This is done by highly predictable and reproducible explosive devices which suddenly open additional gas escape areas (thus causing pressure reduction) and neutralize the thrust by exhausting gases in a direction opposite to that of the motor nozzle. To balance side forces, the thrust termination blow-out devices and their ducts are always designed in symmetrically opposed sets (two or more). In Fig. 1–5 there are four symmetrically placed openings that are blown into the forward dome of the case by circular explosive cords. Two of the sheathed circular cord assemblies are sketched on the outside of the forward dome wall. The ducts that lead the hot gas from these openings to the outside of the vehicle are not shown in this figure. The forward flow of gas occurs only for a very brief period of time, during which the thrust is actually reversed. The rapid depressurization causes a sudden stopping of the combustion at the propellant burning surface. With proper design the explosive cords do not cause a detonation or explosion of the remaining unburned propellant.
2. During some motor development projects it can be helpful to see a partially consumed grain. The motor operation is stopped when the flames are quenched by injecting an inhibiting liquid such as water. Reference 13–12 shows that adding a detergent to the water allows a better contact with the burning surface and reduces the amount of water needed for quenching.
3. *Lowering the combustion pressure* below the pressure deflagration limit. Compared to item 1, this depressurization occurs quite slowly. Many solid propellants have a low-pressure combustion limit of 0.05 to 0.15

MPa. This means that some propellants will not extinguish when vented during a static sea-level test at 1 atm (0.1 MPa) but will stop burning if vented at high altitude.

A sudden depressurization is effective because the primary combustion zone at the propellant surface has a time lag compared to the gaseous combustion zone which, at the lower pressure, quickly adjusts to a lower reaction rate and moves farther away from the burning surface. The gases created by the vaporization and pyrolysis of the hot solid propellant cannot all be consumed in a gas reaction close to the surface, and some will not burn completely. As a result, the heat transfer to the propellant surface will be quickly reduced by several orders of magnitude, and the reaction at the propellant surface will diminish and stop. Experimental results (Chapter 12 of Ref. 13–1) show that a higher initial combustion pressure requires a faster depressurization rate (dp/dt) to achieve extinction.

13.4. COMBUSTION INSTABILITY

There seem to be two types of combustion instability: a set of acoustic resonances or pressure oscillations, which can occur with any rocket motor, and a vortex shedding phenomenon, which occurs only with particular types of grains.

Acoustic Instabilities

When a solid propellant rocket motor experiences unstable combustion, the pressure in the interior gaseous cavities (made up by the volume of the port or perforations, fins, slots, conical or radial groves) oscillates by at least 5% and often by more than 30% of the chamber pressure. When instability occurs, the heat transfer to the burning surfaces, the nozzle, and the insulated case walls is greatly increased; the burning rate, chamber pressure, and thrust usually increase; but the burning duration is thereby decreased. The change in the thrust–time profile causes significant changes in the flight path, and at times this can lead to failure of the mission. If prolonged and if the vibration energy level is high, the instability can cause damage to the hardware, such as overheating the case and causing a nozzle or case failure. Instability is a condition that should be avoided and must be carefully investigated and remedied if it occurs during a motor development program. Final designs of motors must be free of such instability.

There are fundamental differences with liquid propellant combustion behavior. In liquid propellants there is a fixed chamber geometry with a rigid wall; liquids in feed systems and in injectors that are not part of the oscillating gas in the combustion chamber can interact strongly with the pressure fluctuations. In solid propellant motors the geometry of the oscillating cavity increases in size

as burning proceeds and there are stronger damping factors, such as solid particles and energy-absorbing viscoelastic materials. In general, combustion instability problems do not occur frequently or in every motor development, and, when they do occur, it is rarely the cause for a drastic sudden motor failure or disintegration. Nevertheless, drastic failures have occurred.

Undesirable oscillations in the combustion cavity propellant rocket motors is a continuing problem in the design, development, production, and even long-term (10 yr) retention of solid rocket missiles. While acoustically "softer" than a liquid rocket combustion chamber, the combustion cavity of a solid propellant rocket is still a low-loss acoustical cavity containing a very large acoustical energy source, the combustion process itself. A small fraction of the energy released by combustion is more than sufficient to drive pressure vibrations to an unacceptable level.

Combustion instability can occur spontaneously, often at some particular time during the motor burn period, and the phenomenon is usually repeatable in identical motors. Both longitudinal and transverse waves (radial and tangential) can occur. Figure 13–5 shows a pressure–time profile with typical instability. The pressure oscillations increase in magnitude, and the thrust and burning rate also increase. The frequency seems to be a function of the cavity geometry, propellant composition, pressure, and internal flame field. As

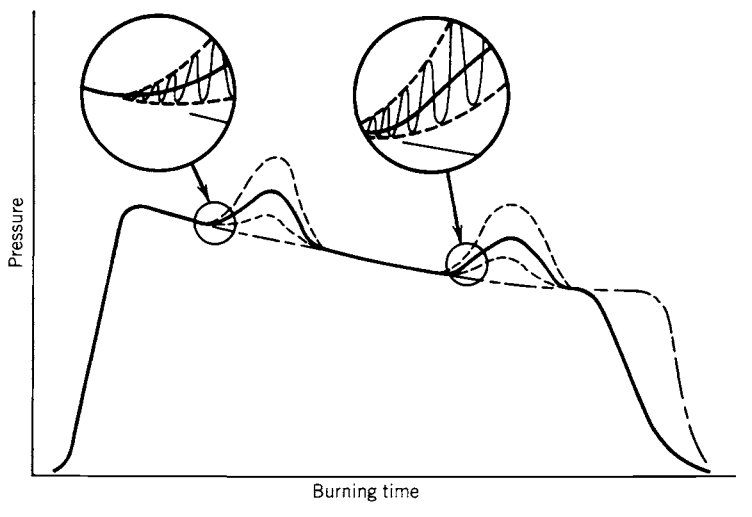

FIGURE 13–5. Simplified diagram showing two periods of combustion instability in the pressure–time history, with enlargements of two sections of this curve. The dashed lines show the upper and lower boundaries of the high-frequency pressure oscillations, and the dot-dash curve is the behavior without instability after a slight change in propellant formulation. The vibration period shows a rise in the mean pressure. With vibration, the effective burning time is reduced and the average thrust is higher. The total impulse is essentially unchanged.

the internal grain cavity is enlarged and local velocities change, the oscillation often abates and disappears. The time and severity of the combustion vibration tend to change with the ambient grain temperature prior to motor operation.

For a simple grain with a cylindrical port area, the resonant transverse mode oscillations (tangential and radial) correspond roughly to those shown in Fig. 9–4 for liquid propellant thrust chambers. The longitudinal or axial modes, usually at a lower frequency, are an acoustic wave traveling parallel to the motor axis between the forward end of the perforation and the convergent nozzle section. Harmonic frequencies of these basic vibration modes can also be excited. The internal cavities can become very complex and can include igniter cases, movable as well as submerged nozzles, fins, cones, slots, star-shaped perforations, or other shapes, as described in the section on grain geometry in Chapter 11; determination of the resonant frequencies of complex cavities is not always easy. Furthermore, the geometry of the internal resonating cavity changes continually as the burning propellant surfaces recede; as the cavity volume becomes larger, the transverse oscillation frequencies are reduced.

The *bulk mode*, also known as the Helmholtz mode, L^* mode, or chuffing mode, is not a wave mode as described above. It occurs at relatively low frequencies (typically below 150 Hz and sometimes below 1 Hz), and the pressure is essentially uniform throughout the volume. The unsteady velocity is close to zero, but the pressure rises and falls. It is the gas motion (in and out of the nozzle) that corresponds to the classical Helmholtz resonator mode, similar to exciting a tone when blowing across the open mouth of a bottle (see Fig. 9–7). It occurs at low values of L^* (see Eq. 8–9), sometimes during the ignition period, and disappears when the motor internal volume becomes larger or the chamber pressure becomes higher. *Chuffing* is the periodic low-frequency discharge of a bushy, unsteady flame of short duration (typically less than 1 sec) followed by periods of no visible flame, during which slow outgassing and vaporization of the solid propellant accumulates hot gas in the chamber. The motor experiences spurts of combustion and consequent pressure buildup followed by periods of nearly ambient pressure. This dormant period can extend for a fraction of a second to a few seconds (Ref. 13–13 and Chapter 13 by Price in Ref. 13–1).

A useful method of visualizing unstable pressure waves is shown in Figs. 9–5 and 13–6 and Ref. 13–14. It consists of a series of Fourier analyses of the measured pressure vibration spectrum, each taken at a different time in the burning duration and displayed at successive vertical positions on a time scale, providing a map of amplitude versus frequency versus burning time. This figure shows a low-frequency axial mode and two tangential modes, whose frequency is reduced in time by the enlargement of the cavity; it also shows the timing of different vibrations, and their onset and demise.

The initiation or triggering of a particular vibration mode is still not well understood but has to do with energetic combustion at the propellant surface. A sudden change in pressure is known to be a trigger, such as when a piece of

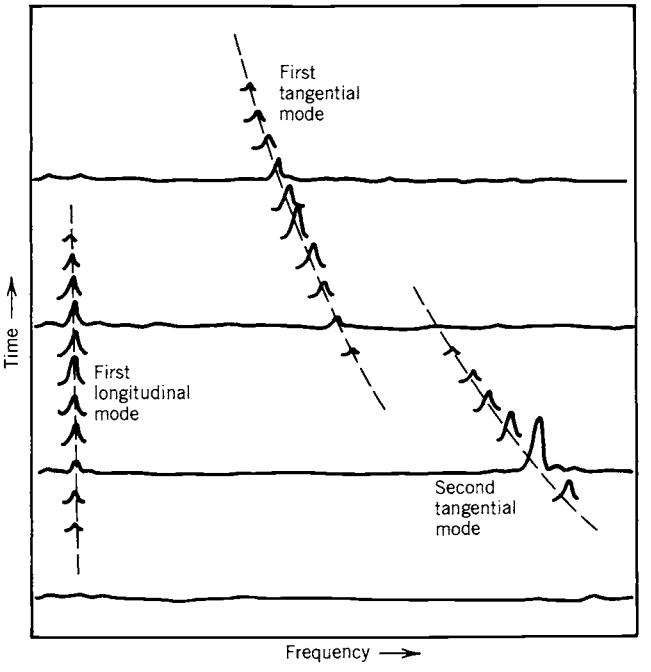

FIGURE 13–6. Example of mode frequency display; also called a "waterfall" diagram of a motor firing. Only four complete time–frequency curves are shown; for easy visualization the other time lines are partly omitted except near the resonating frequencies. The height of the wave is proportional to pressure. As the cavity volume increases, the frequencies of the transverse modes decrease. (Adapted from E. W. Price, Chapter 13 of Ref. 13–1, with permission of AIAA.)

broken-off insulation or unburned propellant flows through the nozzle and temporarily blocks all or a part of the nozzle area (causing a momentary pressure rise).

The shifting balance between amplifying and damping factors changes during the burning operation and this causes the growth and also the abatement of specific modes of vibration. The *response* of a solid propellant describes the change in the gas mass production or energy release at the burning surface when it is stimulated by pressure perturbations. When a momentary high pressure peak occurs on the surface, it increases the instantaneous heat transfer and thus the burning rate, causing the mass flow from that surface to also increase. Velocity perturbations along the burning surface are also believed to cause changes in mass flow. Phenomena that contribute to amplifying the vibrations, or to gains in the acoustic energy (see Ref. 13–1, Chapter 13 by Price), are:

1. The dynamic response of the combustion process to a flow disturbance or the oscillations in the burning rate. This combustion response can be

determined from tests of T-burners as described on pages 533 and 534. The response function depends on the frequency of these perturbations and the propellant formulation. The combustion response may not be in a phase with the disturbance. The effects of boundary layers on velocity perturbations have been investigated in Ref. 13–15.

2. The interactions of flow oscillation with the main flow, similar to the basis for the operation of musical wind instruments or sirens (see Ref. 13–16).
3. The fluid dynamic influence of vortexes.

Phenomena that contribute to a diminishing of vibration or to damping are energy-absorbing processes; they include the following:

1. Viscous damping in the boundary layers at the walls or propellant surfaces.
2. Damping by particles or droplets flowing in an oscillating gas/vapor flow is often substantial. The particles accelerate and decelerate by being "dragged" along by the motion of the gas, a viscous flow process that absorbs energy. The attenuation for each particular vibration frequency is an optimum at a particular size of particles; high damping for low-frequency oscillation (large motors) occurs with relatively large solid particles (8 to 20 μm); for small motors or high-frequency waves the best damping occurs with small particles (2 to 6 μm). The attenuation drops off sharply if the particle size distribution in the combustion gas is not concentrated near the optimum for damping.
3. Energy from longitudinal and mixed transverse/longitudinal waves is lost out through the exhaust nozzle. Energy from purely transverse waves does not seem to be damped by this mechanism.
4. Acoustic energy is absorbed by the viscoelastic solid propellant, insulator, and the motor case; its magnitude is difficult to estimate.

The *propellant characteristics* have a strong effect on the susceptibility to instability. Changes in the binder, particle-size distribution, ratio of oxidizer to fuel, and burn-rate catalysts can all affect stability, often in ways that are not predictable. All solid propellants can experience instability. As a part of characterizing a new or modified propellant (e.g., determining its ballistic, mechanical, aging, and performance characteristics), many companies now also evaluate it for its stability behavior, as described below.

Analytical Models and Simulation of Combustion Stability

Many interesting investigations have been aimed at mathematical models that will simulate the combustion behavior of solid propellants. This was reviewed by T'ien in Chapter 14 of Ref 13–1.

Using complex algorithms and computers it has been possible to successfully simulate the combustion for some limited cases, such as for validating or extrapolating experimental results or making limited predictions of the stability of motor designs. This applies to well-characterized propellants, where empirical constants (such as propellant response or particle-size distribution) have been determined and where the range of operating parameters, internal geometries, or sizes has been narrow. The analytical methods used to date have by themselves not been satisfactory to a motor designer. It is unlikely that a reliable simple analysis will be found for predicting the occurrence, severity, nature, and location of instability for a given propellant and motor design. The physical and chemical phenomena are complex, multidimensional, unsteady, nonlinear, influenced by many variables, and too difficult to emulate mathematically without a good number of simplifying assumptions. However, theoretical analysis gives insight into the physical phenomena, can be a valuable contributor to solving instability problems, and has been used for preliminary design evaluation of grain cavities.

Combustion Stability Assessment, Remedy, and Design

In contrast with liquid rocket technology, an accepted combustion stability rating procedure does not now exist for full-scale solid rockets. Undertaking stability tests on large full-scale flight-hardware rocket motors is expensive, and therefore lower-cost methods, such as subscale motors, T-burners, and other test equipment, have been used to assess motor stability.

The best known and most widely used method of gaining combustion stability-related data is the use of a *T-burner*, an indirect, limited method that does not use a full-scale motor. Figure 13–7 is a sketch of a standard T-burner; it has a 1.5-in. internal diameter double-ended cylindrical burner vented at its midpoint (see Refs. 13–17 to 13–19). Venting can be through a sonic nozzle to the atmosphere or by a pipe connected to a surge tank which maintains a constant level of pressure in the burner cavity. T-burner design and usage usually concentrate on the portion of the frequency spectrum dealing with the transverse oscillations expected in a full-scale motor. The desired acoustical frequency, to be imposed on the propellant charge as it burns, determines the burner length (distance between closed ends).

The nozzle location, midway between the ends of the burner, minimizes attentuation of fundamental longitudinal mode oscillations (in the propellant grain cavity). Theoretically, an acoustic pressure node exists at the center and antinodes occur at the ends of the cavity. Acoustic velocity nodes are out of phase with pressure waves and occur at the ends of the burner. Propellant charges are often in the shape of discs or cups cemented to the end faces of the burner. The gas velocity in the burner cavity is kept intentionally low (Mach 0.2 or less) compared with the velocity in a full-scale motor. This practice minimizes the influence of velocity-coupled energy waves and allows the influence of pressure-coupled waves to be more clearly recognized.

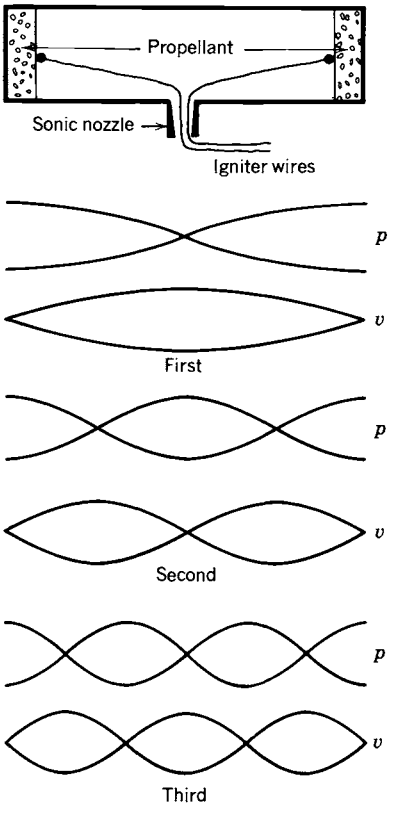

FIGURE 13–7. Standard T-burner and its longitudinal mode standing waves (pressure and velocity).

Use of the T-burner for assessing the stability of a full-scale solid rocket presupposes valid theoretical models of the phenomena occurring in both the T-burner and the actual rocket motor; these theories are still not fully validated. In addition to assessing solid rocket motor combustion stability, the T-burner also is used to evaluate new propellant formulations and the importance of seemingly small changes in ingredients, such as a change in aluminum powder particle size and oxidizer grind method.

Once an instability has been observed or predicted in a given motor, the motor design has to fix the problem. There is no sure method for selecting the right remedy, and none of the cures suggested below may work. The usual alternatives are:

1. Changing the grain geometry to shift the frequencies away from the undesirable values. Sometimes, changing fin locations, port cross-section profile, or number of slots has been successful.

2. Changing the propellant composition. Using aluminum as an additive has been most effective in curing transverse instabilities, provided that the particle-size distribution of the aluminum oxide is favorable to optimum damping at the distributed frequency. Changing size distribution and using other particulates (Zr, Al_2O_3, or carbon particles) has been effective in some cases. Sometimes changes in the binder have worked.
3. Adding some mechanical device for attenuating the unsteady gas motions or changing the natural frequency of cavities. Various inert resonance rods, baffles, or paddles have been added, mostly as a fix to an existing motor with observed instability. They can change the resonance frequencies of the cavities, introduce additional viscous surface losses, but also cause extra inert mass and potential problems with heat transfer or erosion.

Combustion instability has to be addressed during the design process, usually through a combination of some mathematical simulation, understanding similar problems in other motors, studies of possible changes, and supporting experimental work (e.g., T-burners, measuring particle-size distribution). Most solid propellant rocket companies have in-house two- and three-dimensional computer programs to calculate the likely acoustic modes (axial, tangential, radial, and combinations of these) for a given grain/motor, the initial and intermediate cavity geometries, and the combustion gas properties calculated from thermochemical analysis. Data on combustion response (dynamic burn rate behavior) and damping can be obtained from T-burner tests. Data on particle sizes can be estimated from prior experience or plume measurements (Ref. 13–20). Estimates of nozzle losses, friction, or other damping need to be included. Depending on the balance between gain and damping, it may be possible to arrive at conclusions on the grain's propensity to instability for each specific instability mode that is analyzed. If unfavorable, either the grain geometry or the propellant usually have to be modified. If favorable, full-scale motors have to be built and tested to validate the predicted stable burning characteristics. There is always a trade-off between the amount of work spent on extensive analysis, subscale experiments and computer programs (which will not always guarantee a stable motor), and taking a chance that a retrofit will be needed after full-scale motors have been tested. If the instability is not discovered until after the motor is in production, it is often difficult, time consuming, and expensive to fix the problem.

Vortex-Shedding Instability

This instability is associated with burning on the inner surfaces of slots in the grain. Large segmented rocket motors have slots between segments, and some grain configurations have slots that intersect the centerline of the grain. Figure 13–8 shows that hot gases from the burning slot surfaces enter the main flow in

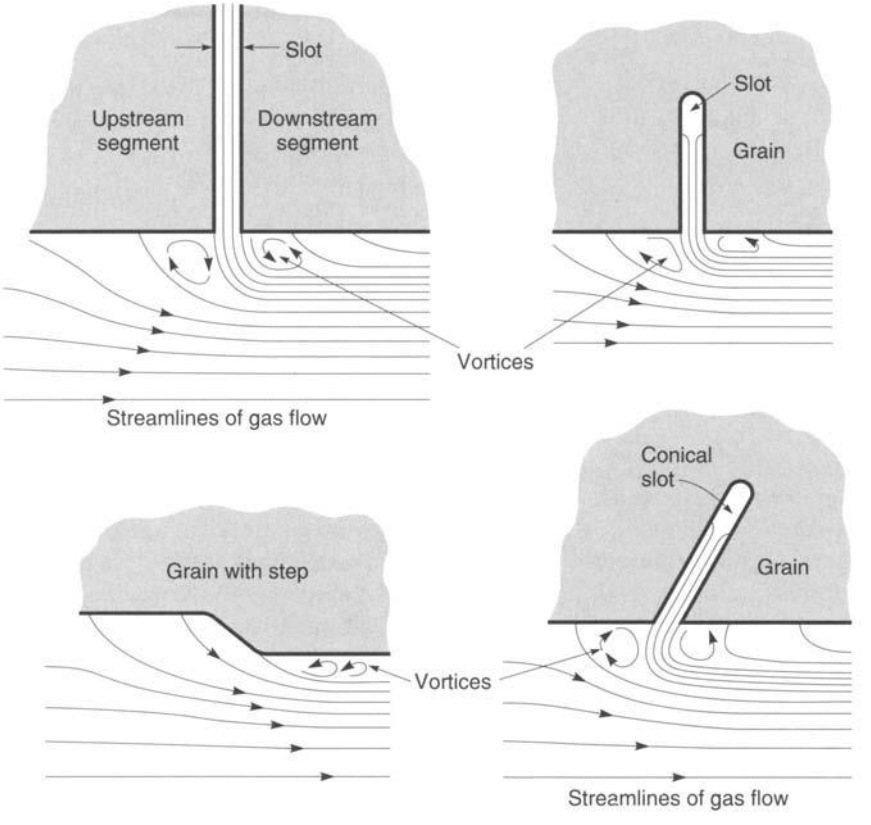

FIGURE 13–8. Simple sketches of four partial grain sections each with a slot or a step. Heavy lines identify the burning surfaces. The flow patterns cause the formation of vortices. The shedding of these vortices can induce flow oscillations and pressure instabilities.

the perforation or central cavity of the grain. The hot gas from the slot is turned into a direction toward the nozzle. The flow from the side stream restricts the flow emanating from the upstream side of the perforation and, in effect, reduces the port area. This restriction causes the upstream port pressure to rise; sometimes there is a substantial pressure rise. The interaction of the two subsonic gas flows causes turbulence. Vortices form and are periodically shed or allowed to flow downstream, thereby causing an unstable flow pattern. The vortex shedding patterns can interact with the acoustic instabilities. Reference 13–21 gives a description and Ref. 13–22 a method for analyzing these vortex-shedding phenomena. The remedy usually is to apply inhibitors to some burning surfaces or to change the grain geometry; for example, by increasing the width of the slot, the local velocities are reduced and the vortices become less pronounced.

PROBLEMS

1. (*a*) Calculate the length of a T-burner to give a first natural oscillation of 2000 Hz using a propellant that has a combustion temperature of 2410 K, a specific heat ratio of 1.25, a molecular weight of 25 kg/kg-mol, and a burning rate of 10.0 mm/sec at a pressure of 68 atm. The T-burner is connected to a large surge tank and prepressurized with nitrogen gas to 68 atm. The propellant disks are 20 mm thick. Make a sketch to indicate the T-burner dimensions, including the disks.
   (*b*) If the target frequencies are reached when the propellant is 50% burned, what will be the frequency at propellant burnout?
   Answers: (*a*) Length before applying propellant = 0.270 m; (*b*) frequency at burnout = 1854 Hz.

2. An igniter is needed for a rocket motor similar to one shown in Fig. 11–1. Igniters have been designed by various oversimplified design rules such as Fig. 13–3. The motor has an internal grain cavity volume of 0.055 m^3 and an initial burning surface of 0.72 m^2. The proposed igniter propellant has these characteristics: combustion temperature 2500 K and an energy release of about 40 J/kg-sec. Calculate the minimum required igniter propellant mass (*a*) if the cavity has to be pressurized to about 2 atm (ignore heat losses); (*b*) if only 6% of the igniter gas energy is absorbed at the burning surface, and it requires about 20 cal/cm^2-sec to ignite in about 0.13 sec.

3. Using the data from Fig. 13–4, plot the total heat flux absorbed per unit area versus pressure to achieve ignition with the energy needed to ignite being just above the deflagration limit. Then, for 0.75 atm, plot the total energy needed versus ignition time. Give a verbal interpretation of the results and trend for each of the two curves.

REFERENCES

13–1. N. Kubota, "Survey of Rocket Propellants and Their Combustion Characteristics," Chapter 1; K. Kishore and V. Gayathri, "Chemistry of Ignition and Combustion of Ammonium-Perchlorate-Based Propellants," Chapter 2; T. L. Boggs, "The Thermal Behavior of Cyclotrimethylene Trinitrate (RDX) and Cyclotetramethylene Tetranitrate (HMX)," Chapter 3; R. A. Fifer, "Chemistry of Nitrate Ester and Nitramine Propellants," Chapter 4; C. E. Hermance, "Solid Propellant Ignition Theories and Experiments," Chapter 5; M. Kumar and K. K. Kuo, "Flame Spreading and Overall Ignition Transient," Chapter 6; E. W. Price, "Experimental Observations of Combustion Instability," Chapter 13; James S. T'ien, "Theoretical Analysis of Combustion Instability," Chapter 14; all in K. K. Kuo and M. Summerfield (Eds), *Fundamentals of Solid-Propellant Combustion*, Volume 90 of Progress in Astronautics and Aeronautics, American Institute of Aeronautics and Astronautics, New York, 1984.

13–2. V. Duterque and G. Lengelle, "Combustion Mechanism of Nitramine-Based Propellant with Additives," *AIAA Paper 88-3253*, July 1988.

13–3. C. Youfang, "Combustion Mechanism of Double-Base Propellants with Lead Burning Rate Catalyst," *Propellants, Explosives, Pyrotechnics*, Vol. 12, 1987, pp. 209–214.

13–4. N. Kubota et al., "Combustion Wave Structures of Ammonium Perchlorate Composite Propellants," *Journal of Propulsion and Power*, Vol. 2, No. 4, July–August 1986, pp. 296–300.

13–5. T. Boggs, D. E. Zurn, H. F. Cordes, and J. Covino, "Combustion of Ammonium Perchlorate and Various Inorganic Additives," *Journal of Propulsion and Power*, Vol. 4, No. 1, January–February 1988, pp. 27–39.

13–6. T. Kuwahara and N. Kubota, "Combustion of RDX/AP Composite Propellants at Low Pressure," *Journal of Spacecraft and Rockets*, Vol. 21, No. 5, September–October 1984, pp. 502–507.

13–7. P. A. O. G. Korting, F. W. M. Zee, and J. J. Meulenbrugge, "Combustion Characteristics of Low Flame Temperature, Chlorine-Free Composite Propellants," *Journal of Propulsion and Power*, Vol. 6, No. 3, May–June 1990, pp. 250–255.

13–8. N. Kubota and S. Sakamoto, "Combustion Mechanism of HMX," *Propellants, Explosives, Pyrotechnics*, Vol. 14, 1989, pp. 6–11.

13–9. L. H. Caveny, K. K. Kuo, and B. J. Shackleford, "Thrust and Ignition Transients of the Space Shuttle Solid Rocket Booster Motor," *Journal of Spacecraft and Rockets*, Vol. 17, No. 6, November–December 1980, pp. 489–494.

13–10. "Solid Rocket Motor Igniters," *NASA SP-8051*, March 1971 (N71-30346).

13–11. I. H. Cho and S. W. Baek, "Numerical Simulation of Axisymmetric Solid Rocket Motor Ignition with Radiation Effect," *Journal of Propulsion and Power*, Vol. 16, No. 4, July–August 2000, pp. 725–728.

13–12. J.Yin and B. Zhang, "Experimental Study of Liquid Quenching of Solid Rocket Motors," *AIAA Paper 90-2091*.

13–13. B. N. Raghunandam and P. Bhaskariah, "Some New Results of Chuffing in Composite Solid Propellant Rockets," *Journal of Spacecraft and Rockets*, Vol. 22, No. 2, March–April 1985, pp. 218–220.

13–14. P. M. J. Hughes and E. Cerny, "Measurement and Analysis of High Frequency Pressure Oscillations in Solid Rocket Motors," *Journal of Spacecraft and Rockets*, Vol. 21, No. 3, May–June 1984, pp. 261–265.

13–15. R. A. Beddini and T. A. Roberts, "Response of Solid Propellant Combustion to the Presence of a Turbulent Acoustic Boundary Layer," *AIAA Paper 88-2942*, 1988.

13–16. F. Vuillot and G. Avalon, "Acoustic–Mean Flow Interaction in Solid Rocket Motors, Using Navier–Stokes Equations," *AIAA Paper 88-2940*, 1988.

13–17. W. C. Andrepont and R. J. Schoner, "The T-Burner Method for Determining the Combustion Response of Solid Propellants," *AIAA Paper 72-1053*, 1972.

13–18. E. W. Price, H. B. Mathes, O. H. Madden, and B. G. Brown, "Pulsed T-Burner Testing of Combustion Dynamics of Aluminized Solid Propellants," *Aeronautics and Astronautics*, Vol. 10, No. 4, April 1971, pp. 65–69.

13–19. R. L. Coates, "Application of the T-Burner to Ballistic Evaluation of New Propellants," *Journal of Spacecraft and Rockets*, Vol. 3, No. 12, December 1966, pp. 1793–1796.

13–20. E. D. Youngborg, J. E. Pruitt, M. J. Smith, and D. W. Netzer, "Light-Diffraction Particle Size Measurements in Small Solid Propellant Rockets," *Journal of Propulsion and Power*, Vol. 6, No. 3, May–June 1990, pp. 243–249.

13–21. F. Vuillot, "Vortex Shedding Phenomena in Solid Rocket Motors," *Journal of Propulsion and Power*, Vol. 11, No. 4, 1995.

13–22. A. Kourta, "Computation of Vortex Shedding in Solid Rocket Motors using a Time-Dependent Turbulence Model," *Journal of Propulsion and Power*, Vol. 15, No. 3, May–June 1999.